

A multi-modal tactile fingertip design for robotic hands to enhance dexterous manipulation

Zhuowei Xu, Zilin Si, Kevin Zhang, Oliver Kroemer, and Zeynep Temel

Abstract—Tactile sensing holds great promise for enhancing manipulation precision and versatility, but its adoption in robotic hands remains limited due to high sensor costs, manufacturing and integration challenges, and difficulties in extracting expressive and reliable information from signals. In this work, we present a low-cost, easy-to-make, adaptable, and compact fingertip design for robotic hands that integrates multi-modal tactile sensors. We use strain gauge sensors to capture static forces and a contact microphone sensor to measure high-frequency vibrations during contact. These tactile sensors are integrated into a compact design with a minimal sensor footprint, and all sensors are internal to the fingertip and therefore not susceptible to direct wear and tear from interactions. From sensor characterization, we show that strain gauge sensors provide repeatable 2D planar force measurements in the 0–5 N range and the contact microphone sensor has the capability to distinguish contact material properties. We apply our design to three dexterous manipulation tasks that range from zero to full visual occlusion. Given the expressiveness and reliability of tactile sensor readings, we show that different tactile sensing modalities can be used flexibly in different stages of manipulation, solely or together with visual observations to achieve improved task performance. For instance, we can precisely count and unstack a desired number of paper cups from a stack with 100% success rate which is hard to achieve with vision only. More details and videos can be found in <https://sites.google.com/view/tactilefingertip>.

I. INTRODUCTION

Robotic manipulation often relies on vision to perceive environmental properties, estimate object poses, and close robot control loops [3], [4]. However, performance degrades when contact regions are occluded by robot manipulators or hidden by clutter [5]. Contact-rich manipulation with robotic hands, such as in-hand object reposing, subtle grasp adjustment, and tool use, frequently exhibit these conditions [6], [7], [8], given the larger enclosure on objects with the multi-finger setting. This limits the effectiveness of robot hand control based solely on vision. Humans compensate for visual occlusion with tactile cues from their hands, where various mechanoreceptors are used to sense pressures, detect slip, and reveal properties of the contact surface [9], [10]. This motivates the deployment of tactile sensing in robotic hands [11].

Despite the development of a variety of tactile sensors [12], [13], [14], [15], [16], [17], [18], [19], developing and deploying tactile sensors for robotic hands presents unique challenges. Robotic hands demand tactile sensors that are compact enough to integrate into fingers without restricting hand’s workspace or mobility. The nature of contact-rich manipulation, where dexterous hands repeatedly make, break, and

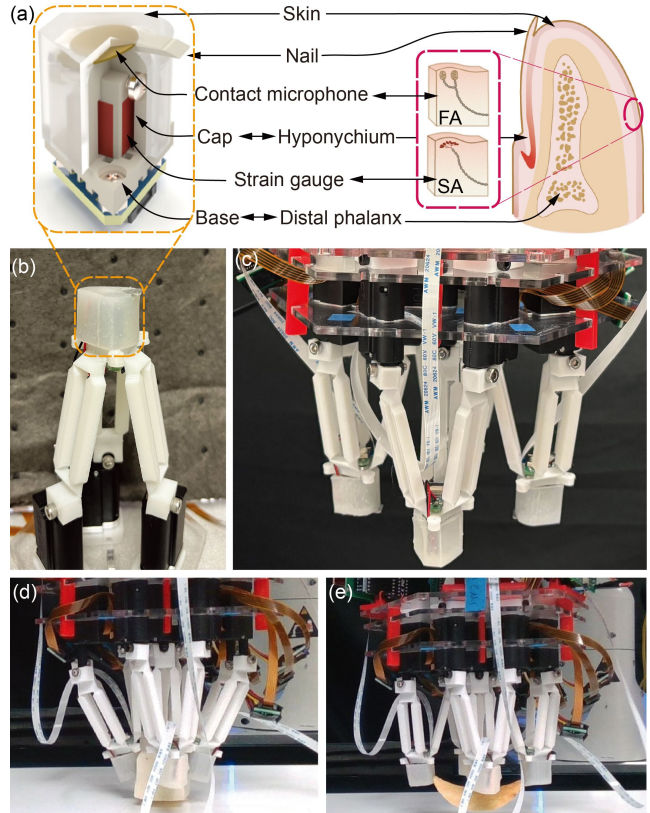


Fig. 1. (a) Fingertip structure includes a rigid bone and a fingernail, and is covered by a soft skin, which mimics human fingertip’s mechanical structure. We leverage strain gauge sensors to emulate the role of slow adapting (SA) mechanoreceptors, responsible for detecting pressure, and a contact microphone sensor to replicate the function of fast adapting (FA) mechanoreceptors, to pick up contact vibrations and infer dynamic contact events such as slip [1]. (b) A Delta finger equipped with the proposed fingertip. (c) A DeltaHand [2] equipped with four tactile fingertips. (d) (e) Grasp a soft tofu cube and a single potato chip without damaging by using tactile sensor measurements in the hand control loop.

switch contacts, requires stable and reliable sensor measurements. Inspired by the richness of human touch, multi-modal tactile sensing can expand hand’s versatility by capturing nuanced contact information such as forces, slippage, and textures. In addition, sensor signals must be expressive and interpretable, enabling effective control of high-DoF robotic hand systems and seamless integration with visual perception.

In this work, we present a multi-modal tactile fingertip that integrates complementary sensing in a compact, hand-compatible design (Fig. 1(a)). We embed strain gauge sensors and a contact microphone sensor in the fingertip structure to capture both force and vibration during contact, reflecting the

two types of mechanoreceptors of human touch. All sensors are internal to the fingertip and therefore prevent direct wear and tear from interactions. Our design is compact (1.9 cm \times 1.9 cm \times 2.7 cm), cost-effective (under \$100), and easy to fabricate (within one hour). Through sensor characterization, we demonstrate that the tactile fingertip can reliably predict 2D planar force and distinguish contact surface properties. By equipping four tactile fingertips on a DeltaHand [2] (Fig. 1(c)), we demonstrate the ease of integration with multi-finger robotic hands and their applications in robotic manipulation.

The main contributions of this work are: (i) a multi-modal tactile fingertip design that integrates force and vibration sensing in a compact form factor, suitable for multi-finger robotic hands; (ii) a systematic characterization on tactile sensors showing that our design provides expressive and reliable sensor measurements; and (iii) evaluation across three manipulation tasks with different levels of visual occlusion to show how different tactile modalities can be flexibly used to mitigate visual occlusion. Experimental results show that our design delivers stable and consistent force measurements that can be directly incorporated into hand control to achieve 100 % success on fragile object pinching (Fig. 1 (d) (e)). Through ablation studies on tasks of unstacking cups and identifying hidden object properties via active touch, we show that vibrotactile signals offer more nuanced and direct contact information which can be easily used to improve task performance with light-weighted data processing and learning when visual cues fall short.

II. RELATED WORK

A. Multi-modal tactile sensor design

To acquire complementary tactile information, researchers have developed multi-modal sensors that integrate different sensing modalities. For example, BioTac [20] employs fluid conduction to sense force, vibration, and temperature, while vision-based sensors such as GelSight [21], [22] capture high-resolution contact geometries and force distributions. More recently, Digit 360 [23] combines optical, pressure, vibrotactile, and temperature sensing in a compact form. Despite their capabilities, vision-based sensors are often bulky and susceptible to skin wear, while fluid-based sensors tend to be costly and require complex manufacturing and signal processing, limiting their integration into robotic hands. In contrast, single-modal force sensors [24], [25], [26] and vibration sensors [19], [27], [28] have been widely adopted for their robustness, sensitivity, and compactness. To leverage the benefits of both modalities, we introduce a simple yet effective multi-modal fingertip that integrates off-the-shelf strain gauge sensors for force sensing with a contact microphone sensor for vibration sensing. This design offers complementary tactile signals for contact-rich manipulation, while remaining low-cost, compact, durable, and easy to integrate, requiring only a one-time calibration.

B. Manipulation with tactile sensing

Tactile sensing plays a dual role in robotic manipulation, serving both as direct feedback for control and as a source of

perceptual features for high-level inference [29]. At the control level, force feedback has been used to guide fingers toward feasible grasp locations [30], and modern approaches often integrate force/torque control with optimization-based motion planning [31]. Tactile and force signals have also supported fine-grained control, such as detecting contact phase transitions for smooth grasping [32], estimating and regulating grip force through slip detection [33], and localizing and manipulating objects in-hand using pressure sensing arrays [34]. At the perceptual level, tactile information can be used to classify object materials [19], or guide robots along restricted structures such as cable routing [35]. Building on these insights, we investigate how force and vibrotactile sensing can enhance manipulation under visual occlusion, either by directly informing control policies or by enabling higher-level tactile perception through active interactions that guide subsequent manipulation steps.

III. METHODOLOGY

We present our fingertip design (Fig. 1 (a)) that integrates functional structures, including a rigid fingernail and soft skin, and two types of tactile sensors, strain gauge sensors and a contact microphone sensor, into a compact fingertip module. The strain gauge sensor and contact microphone sensor are selected as i) they are sensitive to two complementary types of contacts, static forces and vibrotactile information; ii) they are flat and small in scale to be easily integrated into a compact module such as a fingertip; and iii) their sensor readings are interpretable and reliable for robotic hand control.

A. Fingertip design and fabrication

As shown in Fig. 2, the fingertip structure consists of four modules: 1) a triangular base, 2) a semi-compliant square prism, 3) a rigid cap with a rigid fingernail, and 4) a soft skin layer. The triangular base is used to mount a custom Printed Circuit Board (PCB) for sensor data acquisition and as a structural interface to mount the fingertip on the robotic finger. The square prism serves as a rigid bone for mounting the strain gauge sensors. The rigid cap covers the prism with a contact microphone sensor mounted on the top to pick up vibrations from the fingernail. The fingernail extends 1 mm beyond the skin surface to catch the edges of objects. Finally, a soft skin layer covers the whole cap except the fingernail to increase contact friction and enable soft contact, to improve the grasp stability. The overall structure maintains a compact form factor with dimensions of 1.9 cm \times 1.9 cm \times 2.7 cm.

B. Fingertip fabrication

Fig. 2(a) shows the fingertip fabrication procedure. The triangular base and the square prism are 3D printed together using a Raise3D E2 printer. The base is printed with soft TPU, while the prism is printed with a rigid PLA core. The rigid core reduces the hysteresis induced by the soft material to improve the repeatability of the strain gauge sensor measurements. The cap with the fingernail is 3D printed with PLA material on a Bambu Lab printer. After gluing four strain gauge sensors to the prism and a contact sensor on the top of the cap, the cap

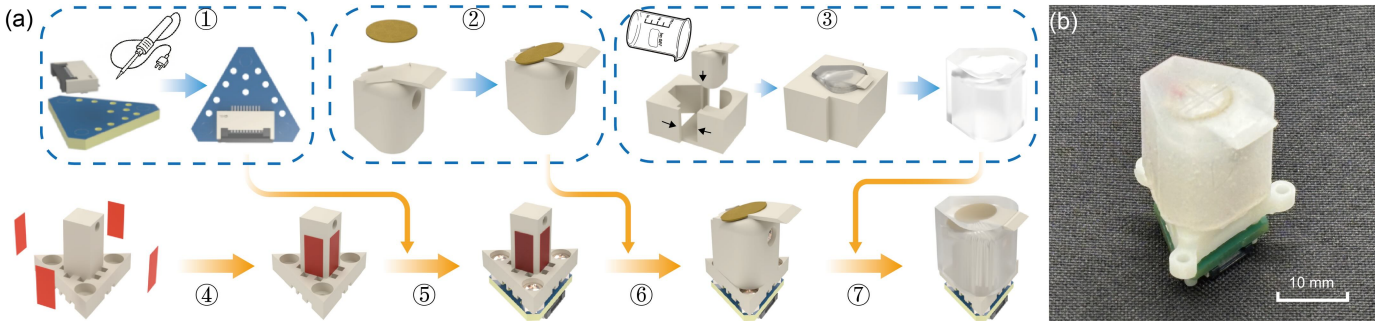


Fig. 2. The fabrication procedure and final prototype of the fingertip. (a) Fingertip fabrication: ① Soldering the connector onto the PCB; ② attaching the contact microphone sensor on the top of the 3D printed cap using super glue; ③ molding a soft skin for the cap with silicone (Mold Star 20T) by using two 3D-printed molds; ④ gluing four strain gauge sensors on each side of the square prism; ⑤ mounting the PCB with M2 screws below the fingertip base; ⑥ Assembling the cap and the base with an M2 screw; ⑦ wearing the soft skin on the cap. (b) A fully assembled fingertip prototype.

is assembled to the prism and secured with an M2 screw. The PCB is then mounted below the base of the fingertip. We mold the soft skin directly over the cap using silicone rubber (Mold Star 20T). The entire process takes around 1 hour (30 mins for silicon curing) and the total cost is less than \$100. Given its ease of fabrication and low cost, our design is scalable and batch-producible to be suitable for multi-finger robotic hands.

C. Strain gauge sensor

We use four strain gauge sensors (BF120-3AA, 4 mm×6.8 mm) to estimate 2D normal forces applied on the lateral surface of the fingertip. The strain gauge sensors are superglued to the four lateral surfaces of the square prism before attaching the cap on it. We use an M2 screw to rigidly secure the cap to the top of the square prism and leave a 1 mm gap on all sides, which allows the prism to bend freely under external contact forces. This deformation induces strain changes in the sensors, which is further transduced into electrical signals. Although it is possible to estimate 3D forces given the four orthogonally arranged strain gauge sensors, in this work we only calibrate and estimate 2D forces to improve the accuracy of force estimation.

D. Contact microphone sensor

To sense the dynamic contact events, we use a piezo disc contact microphone sensor (with 10 mm diameter) to capture the vibrations generated through dynamic contact, such as making and breaking contact, or sliding. The sensor is rigidly attached on top of the fingertip cap, located close to the vibration source, i.e., the fingernail. When the fingernail interacts with an object, the contact vibration is transmitted through the rigid of the cap, captured by the sensor, and then transduced to electrical signals.

E. Read-out circuit

A custom PCB is designed to match the fingertip's footprint, interface with the sensors for data readout. This PCB takes signal inputs from both the strain gauge sensors and the contact microphone sensor and outputs them through a unified output port. The combined signal is then transmitted through a flat

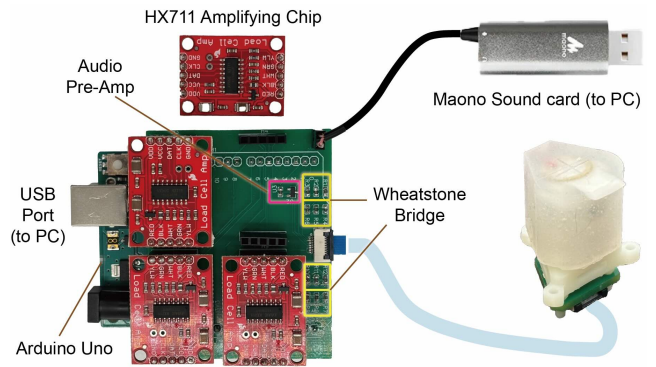


Fig. 3. Readout circuit of the fingertip: the contact microphone sensor signals and the strain gauge sensor signals are collected through the fingertip PCB and carried by an FFC cable to another custom PCB. The strain gauge sensor measurements are amplified and digitized with an HX711 module on an Arduino Uno, while the vibrotactile signals are pre-amplified, digitized by a modified Maono USB sound card. Both are transmitted to the PC via USB.

flexible cable (FFC) for clean and reliable cable routing. The PCB is mounted beneath the fingertip base using M2 screws.

The FFC cable is then connected to another custom PCB (Fig. 3) for sensor reading amplification and analog-to-digital conversion. The signals from the contact microphone are amplified with a preamp. Wheatstone bridges in standard configuration are used to measure the resistance changes of strain gauge sensors and convert them into differential voltage signals. The differential output of the bridge is then fed into an analog-to-digital (ADC) converter (HX711) for signal amplification and analog-to-digital conversion. The resulting digital signals are read out by an Arduino Uno and then transmitted to a computer via the USB interface. The response frequency of the strain gauge sensor and the contact microphone sensor are 15 Hz and 44.1 kHz respectively.

IV. SENSOR CHARACTERIZATION

To demonstrate the capability and precision of the proposed tactile sensors, we performed characterization: i) force estimation with strain gauge sensors and ii) material classification with the contact microphone sensor.

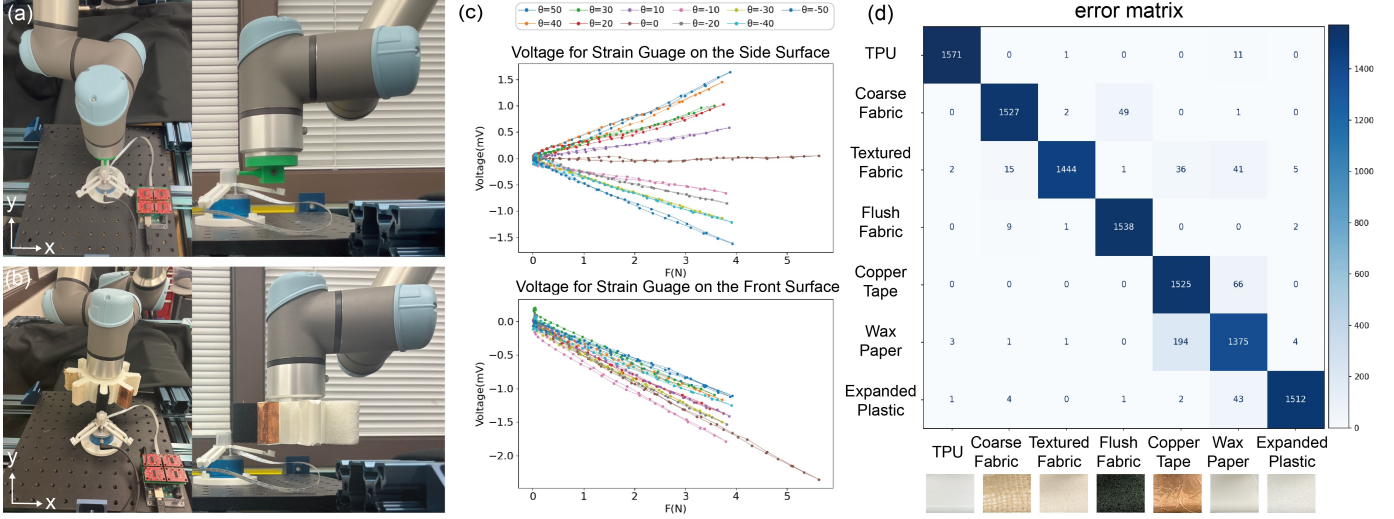


Fig. 4. Tactile sensor characterization setup and results: (a) Front and side views of the setup for strain gauge sensor characterization. A fingertip sits on a 6D force/torque sensor that is rigidly fixed on the table. A UR5e robotic arm with a custom end effector (3 mm cylindrical indenter) is used to step and press on the fingertip from different directions and with incremental indentation depths to characterize 2D planar force sensing. (b) Front and side views of the setup for contact microphone sensor characterization. We use a custom end-effector with samples of seven materials attached on different faces. The UR5e arm is controlled to initiate sliding contacts between the fingernail and a sample to generate vibrotactile signals. (c) We show the linear correspondence between the strain gauge sensor measurements and the ground-truth force readings from 0 to 5 N at a fixed indentation depth across different directions. (d) We learn a material classification model by using vibrotactile measurements. We show the results on the test dataset.

A. Force estimation with strain gauge sensors

We characterize the strain gauge sensors by mapping the raw sensor measurements to estimated forces with a multilayer perceptron (MLP) model. We then evaluate the sensitivity and accuracy of the force estimation. As shown in Fig. 4 (a), the sensor characterization setup consists of a UR5e robotic arm with a customized end-effector (a 3 mm cylindrical indenter) to actively interact with the fingertip. The fingertip is rigidly mounted on top of a 6-DOF force torque sensor (Nordbo NRS-50), which provides the ground-truth forces.

During each trial, the robot followed a predefined trajectory: the end effector incrementally indented the fingertip in the XY plane (Fig. 4 (a)) with a step size of 1.5 mm until a total displacement of 30 mm was reached. Then it retracted along the same path. At each step, the robot paused for 8 seconds to allow the sensor readings to stabilize before recording. This procedure was repeated in a range of orientations in the XY plane (from -50° to 50° in increments of 10°), and at varying contact heights along the Z-axis (from 0 mm to 5 mm in increments of 1 mm), with the fingernail tip defined as the zero reference. To reduce sampling bias and ensure the independence of each trial, indentation angles and contact heights were randomized prior to each run.

As shown in Fig. 4(c), regardless of whether the strain gauge sensors are parallel or perpendicular to the force direction, the raw sensor outputs exhibited an approximately linear relationship with the applied forces at each fixed angle. Although hysteresis was observed in both parallel and perpendicular configurations, it did not affect the linearity of the response, indicating reliable force detection. Based on the collected data, we trained an MLP model to capture nonlinearities and angle-

dependent variations, achieving a mean squared error (MSE) of approximately 0.15 N^2 in the test data set, demonstrating accurate force estimation from strain gauge measurements.

B. Material classification with the contact microphone sensor

Contact microphone sensors can pick up the vibration signals generated during dynamic interaction. We characterize the contact microphone sensor's capability of classifying materials based on sliding contact.

We use seven materials including *TPU*, *Expanded Plastic*, *Copper Tape*, *Coarse Fabric*, *Flush Fabric*, *Wax Paper*, and *Textured Fabric*. A customized end-effector is attached to the UR5e arm, with each material mounted on a different face. For each material, the UR5e arm rotates to align with the target face, approaches the fingernail to initiate contact, and then slide vertically for 16 mm while recording vibrotactile signals. In total, 7000 vibrotactile signal sequences are collected for each material. To train the material classification model, the time-domain signals were transformed into frequency-domain spectrograms using Short-Time Fourier Transform (STFT). Then we train a multilayer perceptron (MLP) classifier that takes spectrograms as input and outputs a 7D one-hot encoded vector representing the seven material classes.

Fig. 4(g) shows the classification error matrix on test dataset. The classification model achieved an overall accuracy of 95.49%, demonstrating accurate material discrimination. Most misclassifications occurred between *Copper Tape* and *Wax Paper*, which we hypothesize due to the similarity in their smooth surface textures despite their different material compositions.

V. EXPERIMENTS

A. Overview

We evaluated the proposed tactile fingertips across three manipulation tasks: i) pinching fragile objects with fingertip force control, ii) counting and unstacking paper cups, and iii) detecting the material of hidden objects through shaking to guide subsequent manipulation. The first task examines whether fingertip tactile signals are reliable enough to serve directly as feedback for closing the control loop. The second investigates whether tactile sensing can serve as an alternative to vision under occlusion to improve manipulation performance. The third evaluates the sensitivity and robustness of tactile sensing for material recognition and its effectiveness in informing downstream manipulation.

B. Experimental setup

We equip a DeltaHand [2] with four tactile fingertips, where the strain gauge sensors are calibrated to estimate forces as described in Sec. IV-A. The DeltaHand is mounted on a Franka Emika Panda arm. For all experiments, we used Cartesian position control to control the Franka arm's end effector and joint position control to control the DeltaHand.

C. Tasks

Fragile object pinching with fingertip force control
Manipulating fragile objects is challenging due to the risk of irreversible damage. Although vision can capture geometric features such as object edges and use them to guide position control, force control provides a more reliable and practical approach by directly adapting control strategies based on contact forces, thereby preventing applying excessive force.

Motivated by this, we use force estimation at the fingertips in closed-loop control to grasp fragile objects. We select tofu cubes and potato chips as representative fragile objects which can also clearly indicate success or failure. We start with a calibration of the grasping force from a single demonstration per object: the operator teleoperates the DeltaHand to grasp and lift the object without damage while recording the pinching force F_{th} . Then we use F_{th} as the threshold for the force-based control of grasping: for each test, we command the DeltaHand fingers to step to close until the measured force $F(t)$ reaches F_{th} , then lift the object. Fig. 5 shows an example of tofu pinching and potato chip pinching and the corresponding force readings from the fingertips.

As a vision-based baseline, we use SAM2 [36] to segment the object contour from the in-hand image. Then we use the segmentation mask to specify the grasp locations on the object edge along the direction between two opposite fingers, and command the fingers to close toward the target grasp locations without force feedback.

We evaluated both force-based control and vision-based control with 25 tests per object. Both controllers achieved 100% success rate with both objects. These results show that our tactile fingertips provide detailed contact information and enables a simple force-threshold controller to perform as effectively as vision-based control. Unlike the vision-based

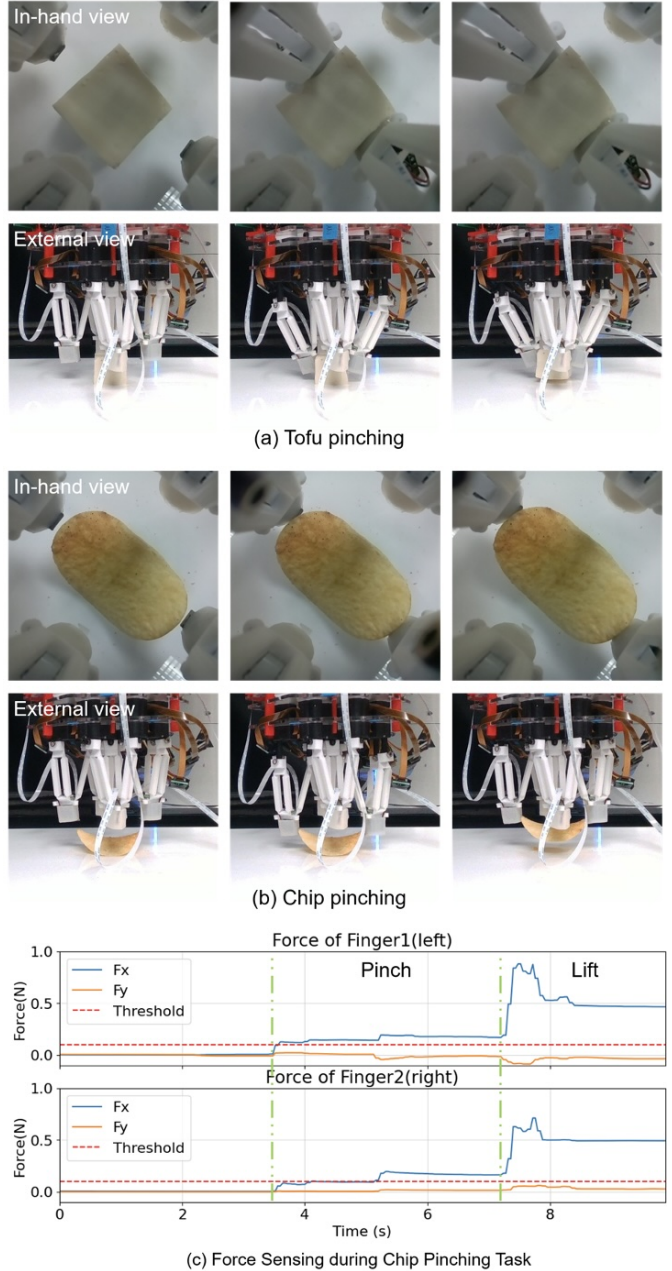


Fig. 5. Pinching and lifting fragile objects including tofu cubes and potato chips with force control based on fingertip strain gauge sensors. We set a force threshold (0.5 N for tofu cubes, and 0.1 N for potato chips) to guide pinching, and maintain the force applied on the object during lifting.

approach, which requires GPU resources to run large pre-trained models (SAM2 runs at 2.5 Hz on an RTX 2080 in our setup), our method operates efficiently on a CPU at 15 Hz, enabling low-latency control and simplifying deployment in resource-constrained settings.

Cup counting and unstacking

Single-view visual perception is often constrained by a limited field of view and occlusion. For example, objects observed by the wrist camera are frequently blocked by the manipulator itself in the view. To address these limitations, complementary sensors can be introduced, such as multi-

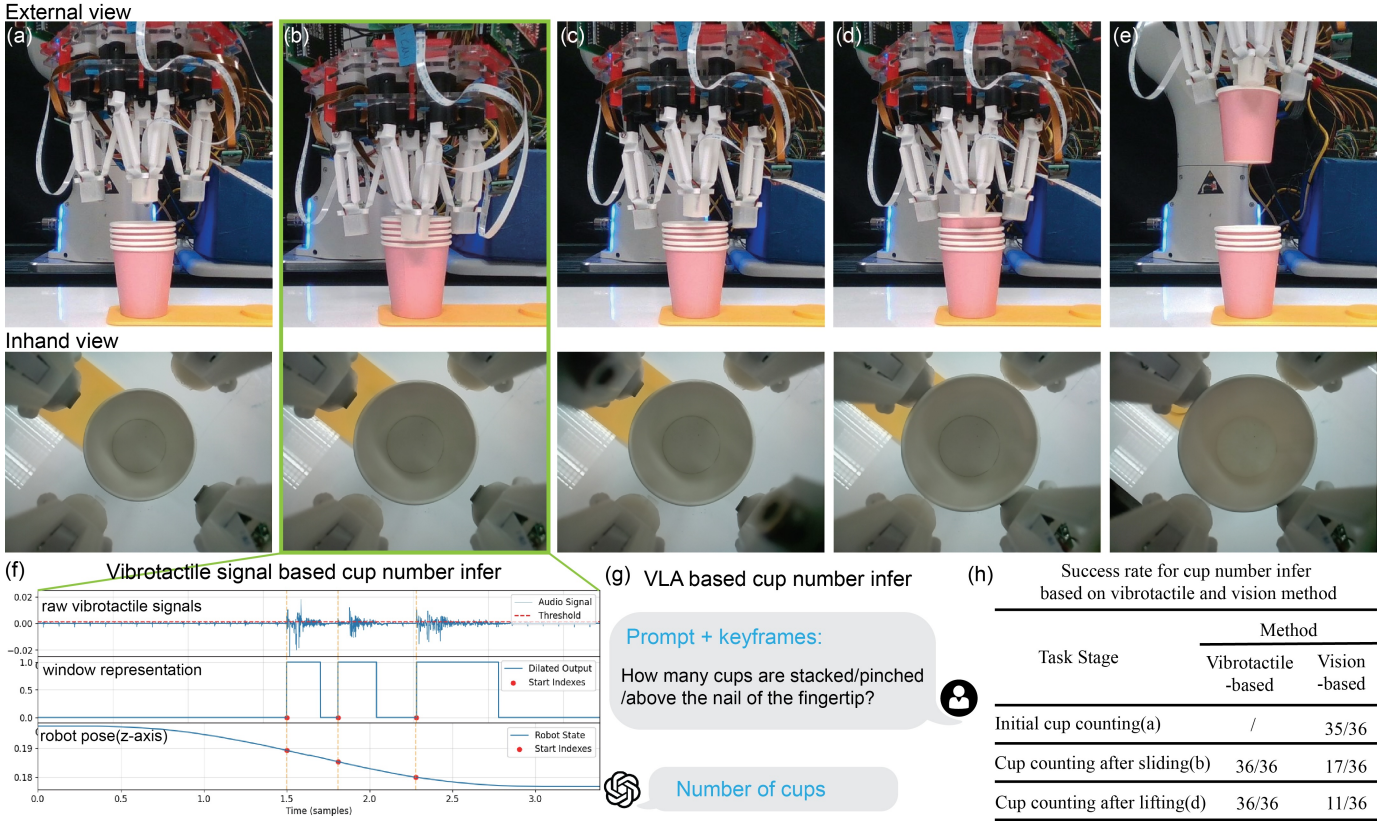


Fig. 6. Cup counting and unstacking pipeline. (a) Start: hand aligned over a cup stack. (b) Moving down to slide through a stack of cup edges. (c) Locate the cup edges based on the vibrotactile features, and move the hand down to the target cup edges location. (d) Close the finger and lift the cups. (e) Separate and unstack the cups. (f) Binarize raw vibrotactile signals to locate the moment of encountering cup edges during sliding, and synchronize with the robot height. (g) vision-based baseline: using text prompts and keyframes from the external camera to query cup counting with a GPT-5 agent. (h) We show vibrotactile-based approach outperforms the vision-based approach, especially with visual occlusion scenarios.

view camera systems or tactile sensors. However, multi-camera setups require additional hardware, calibration, and system integration, thereby increasing the system's overall complexity. In contrast, we employ tactile sensing as a lightweight approach to compensate for partial visual occlusions.

We show how to address partial visual occlusion with our proposed tactile fingertip through a cup counting and unstacking task (Fig. 6). The task begins with the fingernail sliding down a stack of paper cups, during which vibrotactile features are extracted to count the number of cup edges encountered. By combining these vibrotactile features with the robot's Z-axis movement (Fig. 6 (g)), the robot can be commanded to grasp a specified number of cups and lift them to perform unstacking (Fig. 6 (e)). As shown in Fig. 6 (a), counting cups solely from the in-hand camera is infeasible, as all edges except the top one are occluded. In contrast, the vibrotactile signals clearly reveal distinct vibration patterns associated with each cup edge, as illustrated in Fig. 6 (g).

To extract vibrotactile features, we first apply a threshold τ to the time-domain signals, generating a binary sequence $B(t) = \mathbf{1}[I(t) \geq \tau]$. A temporal clustering filter is then employed to merge segments that are separated by small gaps due to signal noise. The onset of each resulting window corresponds to the moment the fingernail encounters a cup edge.

By synchronizing this signal with the robot's motion along the Z-axis, we can determine the robot height associated with each cup edge. During unstacking, given a target number of cups to unstack, the robot moves to the corresponding height, and then the DeltaHand's fingers step to close until reaching a pre-defined force threshold (0.5 N). To overcome inter-cup friction, two opposite fingers alternately move vertically to lift and separate the cups.

We conducted 36 trials to evaluate the accuracy of cup counting and unstacking. In each trial, the initial number of stacked cups is fixed to five, and the robot performed a sliding motion of 21 mm to pass over three cups. Then a target number of cups (one to three) was then randomly selected for lifting. As a vision-based baseline to compare, we employed a GPT-5 VLA agent [37] using text prompts and keyframes from an external camera (Fig. 6(a), (b), and (e)) to query the total number of stacked cups, the number of cups above the fingernail, and the number of cups lifted (Fig. 6(h)). The results are shown in Fig. 6(i). The vibrotactile-based method achieved perfect performance 36/36 in cup counting and lifting. However, while the vision-based method can accurately count the initial stack 35/36, its performance was significantly degraded under occlusion, achieving only 17/36 after sliding and 11/36 after lifting. These results demonstrate

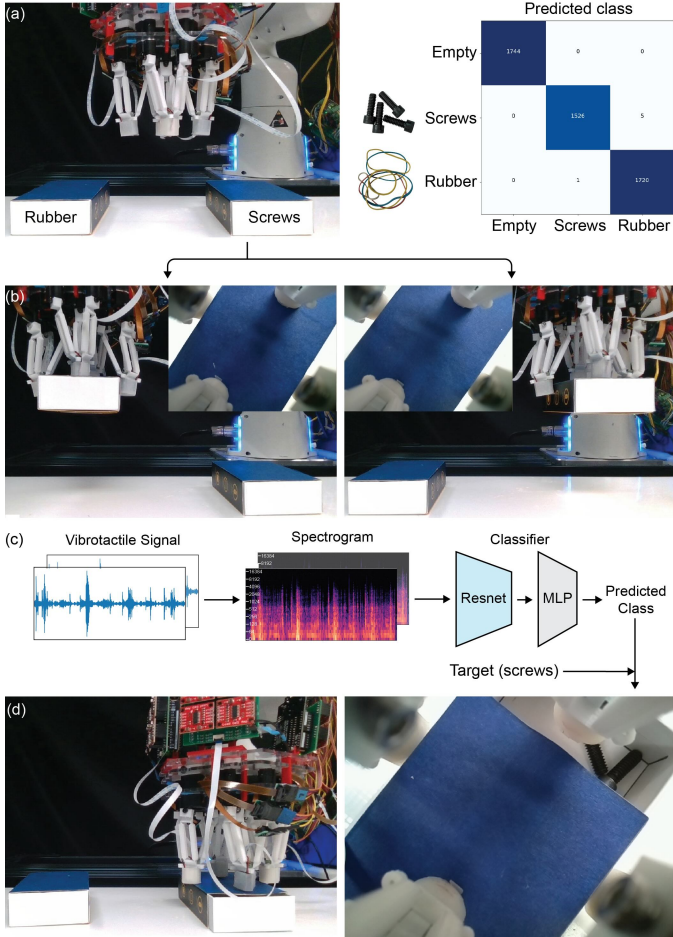


Fig. 7. Experiment setup and pipeline for occluded in-box object material detection and box opening. (a) We offer two boxes, which are visually identical. One box has screws inside and another includes rubber bands, to represent rigid and compliant object. (b) The robot sequentially grasps a box and shake it; (c) the vibrotactile readings collected during shaking are used to predict the hidden material class with a learned model; (d) The robot is guided to select the box that contained the target material class and open it.

that vibrotactile sensing enables robust state estimation and substantially outperforms the visual baseline in scenarios with partial occlusion.

Hidden object detection through shaking

When vision is fully occluded, tactile sensing remains capable of providing contact information for closed-loop control and high-level decision making. To investigate this vision-denied regime, we design a hidden object material inference task (Fig. 7). Given two visually identical boxes, the robot will shake each box and identify the material inside using a vibrotactile-based material classifier. The robot then selects the box with the desired material to open. This task shows how tactile sensing can be used together with active exploration to guide the subsequent manipulation sequence.

We first train a material classification model using vibrotactile data (Fig. 7 (c)) collected through an automated procedure. We set up the task by placing two boxes including screws and rubber bands at pre-defined locations. The Franka arm is

TABLE I
SUCCESS RATES FOR IN-BOX OBJECT INFERENCE UNDER VISION OCCLUSION.

Metric	Screw-filled box	Rubber-band box
Success rate	25/28	28/28

commanded to move to grasp and shake each box in order. We use two opposing fingers of the DeltaHand to grasp the box and press the fingernails against the side of the box to enhance vibration sensing. The arm then lifts the box and performs horizontal shaking at 0.67 Hz with a 5 cm amplitude for 5.6 seconds, during which vibrotactile signals are recorded. This procedure is repeated three times for three classes: a box containing rubber bands, a box containing screws, and an empty grasp. We collect 20 recordings per class. The raw vibrotactile signals are converted into spectrograms using a short-time Fourier transform (STFT), then segmented using a sliding window with the length of 86 to produce 13,319 sequences per class. These sequences are encoded with a ResNet backbone, and fed into an MLP classifier with a 3D one-hot vector output corresponding to the three classes.

During testing, the same shaking procedure is applied. Two visually identical boxes, one containing rubber bands and the other with screws, are placed on the table (Fig. 7(b)). The Franka arm sequentially grasps and shakes each box, during which the trained classification model runs at 10 Hz to continuously predict the in-box material class. After shaking, the final classification is determined by majority voting over all predictions generated during the sequence. Given the predicted labels of both boxes and a user-specified target material (Fig. 7(c)), the robot selects the box containing the target material and opens it by grasping two sides of the box with opposing fingers while using a third finger to slide and push the inner tray outward (Fig. 7(d)).

We evaluated the tasks with 26 trials and show the results in Table I. Overall performance reaches a success rate of 94.64%, indicating that vibrotactile detection can reliably infer in-box materials under fully vision occlusion and effectively offer information for high-level decision making.

VI. CONCLUSIONS

In this work, we present a low-cost, compact, multi-modal tactile fingertip for robotic hands. By integrating strain gauge sensors and a contact microphone sensor, the fingertip provides the sense of contact forces and vibrations. Our characterization results show an accurate estimate of 2D planar forces in the 0–5 N range based on strain gauge sensors and an accuracy of 95.49% in material classification during sliding based on the contact microphone sensor. To demonstrate the functionality of the tactile fingertip, we equipped a *DeltaHand* with four proposed fingertips and evaluated with three manipulation tasks: (i) fragile object pinching with fingertip force control, (ii) cup counting and unstacking, and (iii) hidden object detection through shaking. In the pinching task, a simple force

threshold-based controller achieved 100% success in grasping and lifting tofu cubes and potato chips without damage. We also achieved 100% success in the cup counting and unstacking task by using vibrotactile signals. This shows that vibration sensing is unaffected by self-occlusion or camera viewpoint change and yields stable performance. In the shaking task, we achieved a 94.64% success rate in detecting box contents with vibrotactile signals by shaking, showing that tactile sensing can compensate for visual occlusion. These results indicate that incorporating tactile sensors into robotic hands can complement or even compensate for vision by providing detailed contact information. Tactile sensing not only mitigates the challenges of visual occlusion but also offers more lightweight and practical solutions to guide hand control. Future work will investigate sensor fusion and skill learning that jointly exploit force and vibrotactile cues.

REFERENCES

- [1] E. R. Kandel, J. H. Schwartz, T. M. Jessell, S. Siegelbaum, A. J. Hudspeth, S. Mack *et al.*, *Principles of neural science*. McGraw-hill New York, 2000, vol. 4.
- [2] Z. Si, K. Zhang, O. Kroemer, and F. Z. Temel, “Deltahands: A synergistic dexterous hand framework based on delta robots,” *IEEE Robotics and Automation Letters*, vol. 9, no. 2, pp. 1795–1802, 2024.
- [3] A. Billard and D. Kragic, “Trends and challenges in robot manipulation,” *Science*, vol. 364, no. 6446, p. eaat8414, 2019.
- [4] J. Cui and J. Trinkle, “Toward next-generation learned robot manipulation,” *Science robotics*, vol. 6, no. 54, p. eabd9461, 2021.
- [5] S. Ojha and S. Sakhare, “Image processing techniques for object tracking in video surveillance-a survey,” in *2015 International Conference on Pervasive Computing (ICPC)*. IEEE, 2015, pp. 1–6.
- [6] I. Kao, K. M. Lynch, and J. W. Burdick, “Contact modeling and manipulation,” in *Springer Handbook of Robotics*. Springer, 2016, pp. 931–954.
- [7] M. T. Mason, “Toward robotic manipulation,” *Annual Review of Control, Robotics, and Autonomous Systems*, vol. 1, no. 1, pp. 1–28, 2018.
- [8] Y. Shirai, D. K. Jha, A. U. Raghunathan, and D. Hong, “Tactile tool manipulation,” in *2023 IEEE International Conference on Robotics and Automation (ICRA)*, 2023, pp. 12 597–12 603.
- [9] I. M. Bullock and A. M. Dollar, “Classifying human manipulation behavior,” in *2011 IEEE international conference on rehabilitation robotics*. IEEE, 2011, pp. 1–6.
- [10] C. Papagno, C. Cecchetto, A. Pisoni, and N. Bolognini, “Deaf, blind or deaf-blind: Is touch enhanced?” *Experimental brain research*, vol. 234, no. 2, pp. 627–636, 2016.
- [11] Z. Kappassov, J.-A. Corrales, and V. Perdereau, “Tactile sensing in dexterous robot hands,” *Robotics and Autonomous Systems*, vol. 74, pp. 195–220, 2015.
- [12] P. Svensson, C. Antfolk, A. Björkman, and N. Malešević, “Electrotactile feedback for the discrimination of different surface textures using a microphone,” *Sensors*, vol. 21, no. 10, p. 3384, 2021.
- [13] J. Mejia, V. Dean, T. Hellebrekers, and A. Gupta, “Hearing touch: Audio-visual pretraining for contact-rich manipulation,” in *2024 IEEE International Conference on Robotics and Automation (ICRA)*. IEEE, 2024, pp. 6912–6919.
- [14] M. Kim, J. Yang, D. Kim, and D. Yun, “Soft tactile sensor to detect the slip of a robotic hand,” *Measurement*, vol. 200, p. 111615, 2022.
- [15] G. Chen, S. Tang, S. Xu, T. Guan, Y. Xun, Z. Zhang, H. Wang, and Z. Lin, “Intrinsic contact sensing and object perception of an adaptive fin-ray gripper integrating compact deflection sensors,” *IEEE Transactions on Robotics*, vol. 39, no. 6, pp. 4482–4499, 2023.
- [16] S. Sankar, W.-Y. Cheng, J. Zhang, A. Slepian, M. M. Iskarous, R. J. Greene, R. DeBrabander, J. Chen, A. Gupta, and N. V. Thakor, “A natural biomimetic prosthetic hand with neuromorphic tactile sensing for precise and compliant grasping,” *Science Advances*, vol. 11, no. 10, p. eadr9300, 2025.
- [17] A. Alfadhel, M. A. Khan, S. C. de Freitas, and J. Kosel, “Magnetic tactile sensor for braille reading,” *IEEE Sensors Journal*, vol. 16, no. 24, pp. 8700–8705, 2016.
- [18] Y. Yan, Z. Hu, Z. Yang, W. Yuan, C. Song, J. Pan, and Y. Shen, “Soft magnetic skin for super-resolution tactile sensing with force self-decoupling,” *Science Robotics*, vol. 6, no. 51, p. eabc8801, 2021.
- [19] K. Dai, X. Wang, A. M. Rojas, E. Harber, Y. Tian, N. Paiva, J. Gnehm, E. Schindewolf, H. Choset, V. A. Webster-Wood *et al.*, “Design of a biomimetic tactile sensor for material classification,” in *2022 International Conference on Robotics and Automation (ICRA)*. IEEE, 2022, pp. 10 774–10 780.
- [20] J. A. Fishel and G. E. Loeb, “Sensing tactile microvibrations with the biotac—comparison with human sensitivity,” in *2012 4th IEEE RAS & EMBS international conference on biomedical robotics and biomechatronics (BioRob)*. IEEE, 2012, pp. 1122–1127.
- [21] W. Yuan, R. Li, M. A. Srinivasan, and E. H. Adelson, “Measurement of shear and slip with a gelsight tactile sensor,” in *2015 IEEE International Conference on Robotics and Automation (ICRA)*. IEEE, 2015, pp. 304–311.
- [22] W. Yuan, S. Dong, and E. H. Adelson, “Gelsight: High-resolution robot tactile sensors for estimating geometry and force,” *Sensors*, vol. 17, no. 12, p. 2762, 2017.
- [23] M. Lambeta, T. Wu, A. Sengul, V. R. Most, K. S. Nolan Black, R. Mercado, H. Qi, A. Sohn, B. Taylor, N. Tydingco, G. Kammerer, D. Stroud, J. Khatha, K. Jenkins, K. Most, N. Stein, R. Chavira, T. Craven-Bartle, E. Sanchez, Y. Ding, J. Malik, and R. Calandria, “Digitizing touch with an artificial multimodal fingertip,” in *arXiv*, 2024.
- [24] Y. Jung, D.-G. Lee, J. Park, H. Ko, and H. Lim, “Piezoresistive tactile sensor discriminating multidirectional forces,” *Sensors*, vol. 15, no. 10, pp. 25 463–25 473, 2015.
- [25] R. Koiva, M. Zenker, C. Schürmann, R. Haschke, and H. J. Ritter, “A highly sensitive 3d-shaped tactile sensor,” in *2013 IEEE/ASME international conference on advanced intelligent mechatronics*. IEEE, 2013, pp. 1084–1089.
- [26] A. El-Azizi, S. Islam, P. Piacenza, K. Jiang, I. Kymmissis, and M. Ciocarlie, “Compact led-based displacement sensing for robot fingers,” *arXiv preprint arXiv:2410.03481*, 2024.
- [27] M. J. Yang, J. Cho, H. Chung, K. Park, and J. Kim, “Touch classification on robotic skin using multimodal tactile sensing modules,” in *2023 IEEE International Conference on Robotics and Automation (ICRA)*. IEEE, 2023, pp. 9917–9923.
- [28] E. T. Chang, R. Wang, P. Ballantine, J. Xu, T. Smith, B. Coltin, I. Kymmissis, and M. Ciocarlie, “An investigation of multi-feature extraction and super-resolution with fast microphone arrays,” in *2024 IEEE International Conference on Robotics and Automation (ICRA)*. IEEE, 2024, pp. 3388–3394.
- [29] Q. Li, O. Kroemer, Z. Su, F. F. Veiga, M. Kaboli, and H. J. Ritter, “A review of tactile information: Perception and action through touch,” *IEEE Transactions on Robotics*, vol. 36, no. 6, pp. 1619–1634, 2020.
- [30] R. Fearing, “Simplified grasping and manipulation with dexterous robot hands,” *IEEE Journal on Robotics and Automation*, vol. 2, no. 4, pp. 188–195, 2003.
- [31] L. Righetti, M. Kalakrishnan, P. Pastor, J. Binney, J. Kelly, R. C. Voorhies, G. S. Sukhatme, and S. Schaal, “An autonomous manipulation system based on force control and optimization,” *Autonomous Robots*, vol. 36, no. 1, pp. 11–30, 2014.
- [32] R. D. Howe, N. Popp, P. Akella, I. Kao, and M. R. Cutkosky, “Grasping, manipulation, and control with tactile sensing,” in *Proceedings., IEEE International Conference on Robotics and Automation*. IEEE, 1990, pp. 1258–1263.
- [33] M. R. Tremblay and M. R. Cutkosky, “Estimating friction using incipient slip sensing during a manipulation task,” in *[1993] Proceedings IEEE International Conference on Robotics and Automation*. IEEE, 1993, pp. 429–434.
- [34] Y. Chebotar, O. Kroemer, and J. Peters, “Learning robot tactile sensing for object manipulation,” in *2014 IEEE/RSJ International Conference on Intelligent Robots and Systems*. IEEE, 2014, pp. 3368–3375.
- [35] A. Wilson, H. Jiang, W. Lian, and W. Yuan, “Cable routing and assembly using tactile-driven motion primitives,” *arXiv preprint arXiv:2303.11765*, 2023.
- [36] N. Ravi, V. Gabeur, Y.-T. Hu, R. Hu, C. Ryali, T. Ma, H. Khedr, R. Rädle, C. Rolland, L. Gustafson *et al.*, “Sam 2: Segment anything in images and videos,” *arXiv preprint arXiv:2408.00714*, 2024.
- [37] OpenAI. (2025) Chatgpt. [Accessed: 2025-09-15]. [Online]. Available: <https://chat.openai.com/>